






# Warming induced changes in wood matter accumulation in tracheid walls of spruce

Elena BABUSHKINA\*  <http://orcid.org/0000-0002-1355-4307>;  e-mail: babushkina70@mail.ru

Dina ZHIRNOVA<sup>1</sup>  <http://orcid.org/0000-0002-5189-5700>; e-mail: dina-zhirnova@mail.ru

Liliana BELOKOPYTOVA<sup>1</sup>  <http://orcid.org/0000-0002-8475-7304>; e-mail: white\_lili@mail.ru

Eugene VAGANOV<sup>2, 3</sup>  <https://orcid.org/0000-0001-9168-1152>; e-mail: eavaganov@hotmail.com

<sup>1</sup> Khakass Technical Institute, Siberian Federal University, Abakan, 655017, Russia

<sup>2</sup> Siberian Federal University, Krasnoyarsk, 660041, Russia

<sup>3</sup> Sukachev Institute of Forest, Siberian Branch of Russian Academy of Sciences, Krasnoyarsk, 660036, Russia

## Acknowledgements

Authors would like to thank administration of the National Park “Shushensky Bor” and personally its director Tolmachev V.A. for providing permission and facilitating field work on the park territory. The research reported in this manuscript is funded by the Russian Foundation for Basic Research (project no. 17-04-00315).

**Abstract:** The warming-driven increase of the vegetation season length impacts both net productivity and phenology of plants, changing an annual carbon cycle of terrestrial ecosystems. To evaluate this influence, tree growth along the temperature gradients can be investigated on various organization levels, beginning from detailed climatic records in xylem cells' number and morphometric parameters. In this study, the Borus Ridge of the Western Sayan Mountains (South Siberia) was considered as a forest area under rapid climate change caused by massive Sayano-Shushenskoe reservoir. Several parameters of Siberian spruce (*Picea obovata* Ledeb.) xylem anatomical structure were derived from normalized tracheidograms of cell radial diameter and cell wall thickness and analyzed during 50 years across elevational gradient (at 520, 960, and 1320 m a.s.l.). On the regional scale, the main warming by 0.42°C per decade occurs during cold period (November–March). Construction of the reservoir accelerated local warming substantially since 1980, when abrupt shift of the cold season temperature by 2.6°C occurred. It led to the vegetation season beginning 3-6 days earlier and ending 4-10 day later with more stable summer heat supply. Two spatial patterns were found in climatic response of maximal cell wall thickness: (1) temperature has maximal impact during 21-day period, and its seasonality shifts with elevation in tune with temperature gradient; (2) response to the date of temperature passing +9.5°C threshold is observed at two higher sites. Climate change yielded significantly bigger earlywood spruce tracheids at all sites, but its impact on cell wall deposition process had elevational gradient: maximal wall thickness increased by 7.9% at the treeline, by 18.2% mid-range, and decreased by 4.9% at the lower boundary of spruce growth; normalized total cell wall area increased by 6.2-6.8% at two higher sites but remained stable at the lowest one. We believe that these patterns are caused by two mechanisms of spruce secondary growth cessation: “emergency” induced by temperature drop versus “regular” one in warmer conditions. Therefore, autumn lengthening of growth season stimulated wood matter accumulation in tracheid walls mainly in cold environment, increasing role of boreal and mountain forests in carbon cycle.

**Keywords:** Climate change; Sayano-Shushenskoe Reservoir; Elevational gradient; *Picea obovata*; Quantitative wood anatomy; Climate–growth relationship

## Introduction

The warming-driven increase of vegetation season length impacts both net productivity and phenology of plants, and these shifts in turn influence an annual carbon cycle of terrestrial ecosystems (Churkina et al. 2005; Davi et al. 2006; Peñuelas and Filella 2009; Körner and Basier 2010; Castagneri et al. 2018). For

example, depending on species and region, phenological events are reported to occur 2-5 days per decade earlier in spring and 1-3 days per decade later in autumn, probably due to photoperiod-driven restraints (Keeling et al. 1996; Menzel 2000; Root et al. 2003; Stinziano and Way 2014; Ma et al. 2018; Wang et al. 2018). Longer growth season leads to an increase in annual vegetation productivity or compensates for the mid-summer reduction in carbon sequestration caused by rising temperatures and drought stress (Badeck et al. 2004; Davi et al. 2006; Keenan et al. 2014; Stinziano and Way 2014); however, divergent rates of warming and phenological shifts in autumn may lead to carbon losses (Piao et al. 2008).

To evaluate impact of a temperature increase on the forest ecosystems as one of the main carbon sinks, different approaches can be used. Research of trees reaction in controlled conditions (e.g. in isolated chambers) allows to model any possible change of the environment, but such experiments as a rule are performed on young trees up to saplings, have time limitation of one or several years, and their results are often reliable only within the observation range (Peltola et al 2002; Kilpeläinen et al 2003; Wolkovich et al. 2012; Taeger et al. 2015). On the other hand, comparative analysis of growth patterns and climatic response of trees observed along the temperature gradient (latitudinal or altitudinal) in the field under natural conditions provides an assessment of an actual climatic variation and current trends (Price et al. 2013; Case and Duncan 2014; Wieser et al. 2014; Schickhoff et al. 2015; Malanson 2017; Babushkina et al. 2018a); however, complexity of several changing environmental factors and their interaction hampers estimation of impact provided by any single factor, for example air temperature (Hänninen and Tanino 2011). In this case, the main indicators of woody plants' productivity are radial growth, wood density, and other tree-ring parameters registering its dynamics during all tree lifespan (Fritts 1976; Vaganov et al. 1985, 2006; Schweingruber 1988). The results of experiments and observations are inconsistent; there is evidence of both positive changes and nonsignificant response of growth and wood density as carbon storage indicators (Kilpeläinen et al, 2003; Skomarkova et al. 2006; Chave et al. 2009).

Reaction of plants on the temperature increase includes responses on several levels of organization: from cell through tissue and organism to population and ecosystem (Fritts 1976; Fritts and Swetnam 1989; Schweingruber 2006; Vaganov et al. 2006; Fonti et al. 2010). Evidently, each next level integrates results of the previous one (Leuzinger et al. 2011). For example, xylem cells of the tree stem record climatic conditions during growth season in their production (number) and morphometric parameters, and on the tissue level these parameters are integrated in form of annual ring width and its density (Plomion et al. 2001; Vaganov et al. 2006). It means that regulation of xylogenesis' seasonal kinetics by shifts of the seasonal climatic cycle is also reflected throughout tree lifespan in the xylem anatomical parameters (Gričar et al. 2015; Carrer et al. 2017; Deslauriers et al. 2017). It should be noted that with wood density, cell wall thickness or area are better indicators of woody biomass production than cell production or tree-ring width (Cuny et al. 2015).

At the end of the 1970s, a great dam was built and the massive Sayano-Shushenskoe reservoir was created in the Western Sayan Mountains (South Siberia). It modified thermal regime of the area adjacent to the reservoir, especially near the dam itself. Most evident changes have concerned the vegetation season length extending by 8-10 days and winter temperatures increasing by ca. 4°C (comparing 40 years before and after 1980), the latter being more than twice of regional warming trend (Babushkina et al. 2018a). The Borus Ridge is located in the immediate vicinity of the dam, and most of its elevation is covered by mixed conifer forests ranging from the forest-steppes at the foothills (ca. 300 m a.s.l.) to the treeline ecotone at ca. 1400 m a.s.l. This wide range of forest habitats can be applied to individual tree species too; particularly, Siberian spruce (*Picea obovata* Ledeb.) can be found from 500 m a.s.l. to the treeline. Therefore, this area can be considered as some long-term anthropogenic experiment of the forest exposed to rapid warming. Dendrochronological research showed stable radial growth and successful acclimation of the considered spruce stands (Babushkina et al. 2018a); however, carbon sequestration by trees may be also modulated by change of wood density. We expect that wood anatomy may reveal finer details of woody biomass production dynamics under such conditions. As latewood is the most dense zone of tree ring, we hypothesize that local climate change may be reflected mainly in the latewood cell wall thickness increase due to autumn warming.

In this study we focused on those shifts of tree-ring anatomical structure, which: (a) have clear response to the warming influence of the reservoir; (b) record differences of climatic variables before and after the dam construction in more details; (c) are based on fundamental parameters (radial diameter and wall thickness of cells) of the xylem anatomical structure, adequately reflecting processes of its development;

(d) allow to assess the warming-induced increase of the wood substance accumulation.

## 1 Materials and Methods

### 1.1 Study area and data sources

The research was carried out on the Borus Ridge of the Western Sayan Mountains, which is located east of the dam of the Sayano-Shushenskoe reservoir and at the south boundary of the Minusinsk Depression. Wide altitudinal range from 300 to 2300 m a.s.l. ensures high variety of vegetation cover, but most of the ridge area is covered by conifer forests represented by *Pinus sylvestris*, *P. sibirica*, *Larix sibirica*, *Picea obovata*, and *Abies sibirica*. Soils are loamy, thin and stony, with numerous rock outcrops. Climate of the study area is sharply continental and has high daily and seasonal temperature variation. Precipitation has maximum in July and minimum in February–March. The temperature decreases with elevation; on the contrary, precipitation amount has positive elevational trend, especially in winter (in northern part of Western Sayan, annual precipitation increases by 100–200 mm per 100 m, Polikarpov and Nazimova 1963; also see Babushkina et al. 2018a for comparison of precipitation and temperature at Cheryomushki with Olenya Rechka station at 1400 m a.s.l.).

Construction of the Sayano-Shushenskoe reservoir (area 620 km<sup>2</sup>; depth up to 220 m) immensely influenced local climate of the last decades. The dam construction started in 1968, and the bed of the Yenisei River was blocked in October 1975. The first three turbines of the power plant were launched in the end of 1979, and the rest seven turbines were launched during 1980–1985. The reservoir was filled to the planned mark first time in 1990 (Popov and Shatravskii 1994).

In this study we used daily and monthly series of average air temperature observed at the Cheryomushki weather station (Cher, 1951–2014, 52.87°N 91.42°E, 330 m a.s.l.) located at the Yenisei riverbank 5 km downstream from the dam. To assess quantitatively impact of the reservoir, its dam, and the power plant on the local climate, series from the Cheryomushki station were compared with regional series (Reg) calculated by averaging monthly series from two weather stations: Minusinsk (53.70°N 91.70°E, 250 m a.s.l.) and Tashtyp (52.72°N 89.88°E, 450 m a.s.l.). These stations were chosen for two reasons: (1) longer series length than Cheryomushki and (2) location in the Minusinsk Depression in ca. 90–100 km from the reservoir on relatively similar elevations. The comparison was performed for temperatures averaged during warm season (April–October, when monthly  $T > 0^{\circ}\text{C}$  near the dam), and cold season (November–March,  $T < 0^{\circ}\text{C}$ ). For detailed analysis of temperature intra-annual dynamics, daily data from Cheryomushki were smoothed by moving average with 21-day window width and 1-day step.

Cores of *Picea obovata* trees were collected within 10 km from the dam from three sampling sites located at different elevations (Babushkina et al. 2018a, 2019) in vicinity of the Talovka stream (small tributary of the Yenisei River): LOW (52.83°N 91.45°E, ca. 520 m a.s.l.); MID (52.80°N 91.48°E, ca. 960 m a.s.l.); HIGH (52.81°N 91.51°E, ca. 1320 m a.s.l.). The sampling sites were selected on the territory of the National Park “Shushensky Bor”, which minimizes direct human impact on the forests. At the site selected on the lower distribution limit of spruce (LOW), the tree stand consists mainly of fir, birch and spruce (ca. 30%) with some trees of Scots and Siberian pine; most of spruce trees grow alongside the stream and higher on the northern slope. The MID site is covered by Siberian pine stand with Scots pine and spruce trees (ca. 10%) growing on the slopes of small valley on the northern macroslope. On the upper treeline (HIGH), most of tree stand is also represented by Siberian pine; spruces (ca. 10%) grow near the stream and on the stony eastern slope.

### 1.2 Sampling and processing of dendrochronological data

For sampling, dominant and subdominant mature healthy living trees were selected. Cores were sampled with an increment borer at the breast height (ca. 1.3 m). Cores transportation and storage were performed with classical dendrochronological techniques (Cook and Kairiukstis 1990). We selected 5 cores from each site for anatomical measurements. Selection was performed subjectively, preferring cores without mechanical damage and trees above 100 years old (LOW: cambial age at the breast height in 2014 is 89–106 yr, DBH = 16–35 cm; MID: cambial age 120–131 yr, DBH = 14–22 cm; HIGH: cambial age 95–138 yr,

DBH = 10–25 cm). It allowed us to exclude from consideration juvenile wood, minimizing size- and age-related trends and differences between trees/sites in the anatomical parameters of tree rings during analyzed period (Vysotskaya and Vaganov 1989; Lei et al. 1996; Eilmann et al. 2009). Thin cross-sections (15–20  $\mu\text{m}$ ) were cut with a sliding microtome and stained with safranin (1% solution in ethanol). Then, we dehydrated the cross-sections using ethanol solutions with increasing concentrations, washed with xylol, and permanently preserved in Canada balsam. Microphotographs of prepared sections were captured with a digital camera mounted on an optical microscope with 200 $\times$  magnification.

Anatomical measurements were performed in Lineyka program (Silkin 2010) for 1965–2014 (the last 50 years of tree growth). The following parameters were measured: cell number ( $N$ ), lumen radial diameter ( $LD$ ) and double cell wall thickness ( $DWT$ ) of each cell to within 0.01  $\mu\text{m}$  (Vaganov et al. 1985; Larson 1994), five radial files of tracheids were measured in each ring (Seo et al. 2014; Belokopytova et al. 2019). Then corresponding intra-annual series (tracheidograms) of cell radial diameter ( $D = LD + DWT$ ) and single cell wall thickness ( $CWT = DWT/2$ ) were calculated. To provide comparability of radial files and rings with different cell number, all tracheidograms were normalized (stretched or compressed) to the same number  $N = 15$  (Online Resource 1; Panyushkina et al. 2003; Ziaco and Biondi 2016; Belokopytova et al. 2019). Then measurements of all five radial files were averaged for each tree ring. Maximal cell wall thickness ( $CWT_{max}$ ) was determined from  $CWT$  normalized tracheidogram of each ring. Cell wall area was calculated using both  $D$  and  $CWT$  normalized tracheidograms under assumption of rectangular cell shape:  $CWA = D \cdot T - LD \cdot (T - DWT)$ , where value  $T = 27 \mu\text{m}$  was applied for cell tangential diameter, because measurements for randomly selected rings at all three sites showed its normal distribution around this value (Online Resource 1). After that, total cell wall area was summarized from all 15 normalized cells:  $\Sigma CWA = \sum_{n=1}^{15} CWA$ . Wood density was calculated for each normalized cell (assumed to be rectangular) as  $\rho = \rho_0 \cdot CWA / (D \cdot T)$ , where  $\rho_0 = 1.53 \text{ g/cm}^3$  is wood matter density (Stamm 1929), and then weighted average density was calculated for the ring taking into account different areas of cells:  $\rho_{mean} = \sum_{n=1}^{15} (\rho \cdot D \cdot T) / \sum_{n=1}^{15} (D \cdot T) = \sum_{n=1}^{15} (\rho \cdot D) / \sum_{n=1}^{15} D$ . Site chronologies of  $CWT_{max}$ ,  $\Sigma CWA$ , and  $\rho_{mean}$  were obtained by averaging respective series of all five trees at each site. Robustness statistics of these chronologies are typical for anatomical parameters (Online Resource 1). EPS is below 0.85, but it is expected for anatomical parameters' chronologies even with larger sample size (e.g., 12 trees and large number of measured radial files in Carrer et al. 2017).

### 1.3 Statistical analysis

In this study arithmetic mean (*mean*) and standard deviation (*stdev*) were used. Closeness of relationships between time series was evaluated with Pearson's correlation coefficients. Also time series of differences between two variables were calculated and used in comparative analysis of local / regional temperature, tree-ring parameters' dynamics at different elevations. When differences in means for two time series or two parts of one time series were analyzed, a significance level was evaluated with two-tailed *t*-test, as well as for correlations. Long-term trends were modeled with simple linear regression.

Climate change and its influence on cell wall deposition were investigated using two approaches: (1) long-term trends in chronologies of anatomical traits related to this process and in climatic parameters important for them; (2) comparison of sub-periods before and after the dam construction by calculating *mean*  $\pm$  *stdev* and significance of difference in means for the same anatomical and climatic series.

## 2 Results

### 2.1 Regional and local climatic dynamics

Long-term warming was observed in the whole region, especially during cold period, but it occurred substantially faster in the vicinity of the reservoir (Figure 1). Comparison of local and regional temperature dynamics showed that very abrupt shift of local climate happened in the cold season temperatures between 1979 and 1980. Therefore, all period of instrumental climatic observations at the Cheryomushki station was divided into two sub-periods: 1951–1979 and 1980–2014. Comparison of sub-periods showed that regional mean temperatures of cold season increased from  $-13.5 \pm 1.9^\circ\text{C}$  to  $-12.0 \pm 2.0^\circ\text{C}$  (*mean*  $\pm$  *stdev*), whereas

local temperatures undergone much further increase from  $-10.6 \pm 2.0^{\circ}\text{C}$  to  $-6.5 \pm 1.7^{\circ}\text{C}$ . During warm season, both local and regional warming was slower: from  $+10.6 \pm 0.6^{\circ}\text{C}$  to  $+11.2 \pm 0.6^{\circ}\text{C}$  in the region and from  $+11.2 \pm 0.5^{\circ}\text{C}$  to  $+11.9 \pm 0.6^{\circ}\text{C}$  near the dam. All differences in means between the sub-periods were significant at the level  $p < 0.05$ . Correlations between local and regional seasonal temperature series were 0.95-0.98 for separate sub-periods; during all 1951-2014 period the correlation remained high for the warm season ( $r = 0.95$ ) but decreased for the cold one ( $r = 0.87$ ).

Comparison of intra-annual temperature dynamics before and since 1980 showed that warming was maximal in winter, summer temperatures were stable (Figure 2). At the dam elevation, onset of the vegetation season shifted to the earlier dates by 4-6 days, and its offset occurred 4-10 days later (depending on temperature threshold value). Taking into account temperature lapse in mountains, seasonality shift had different values depending on site elevation, but persistent direction of the vegetation season lengthening both in spring and in autumn.

## 2.2 Reaction of the spruce tree-rings structure on local climate shift

Comparative analysis of normalized tracheidograms averaged for the two sub-periods (Figure 3) showed that since 1980 the spruce anatomical structure had significantly changed at all elevations. Earlywood tracheids became larger, especially at the LOW site, but size increase of latewood cells was significant only in the middle of the spruce elevational distribution range. Cell wall thickness increased in the upper half of the spruce range, especially in latewood. As for derivative anatomical traits, increase of cell wall area was observed for the most cells of tree ring at the MID and HIGH sites, whereas at the LOW site it occurred only in earlywood. Density dynamics also had an elevational gradient: substantial increase was observed for the most part of tree ring at the upper treeline; increase was significant only for last cells in the mid-range stand (MID); and density decreased for the most part of tree ring at the lower boundary of the spruce range.

## 2.3 Response of the maximum cell wall thickness to the end-of-season temperature and date of growth season ending

Previous research (Babushkina et al. 2019) showed that for Siberian spruce in the study area, response of *CWTmax* on the end-of-season temperature was positive across the whole elevational range of distribution (500-1350 m a.s.l.). These dendroclimatic correlations were calculated for 21-day moving average temperature series (Figure 4; see also verification of the optimal window width of the temperature series in Online Resource 2). Maximum correlation coefficient values were observed with elevation-driven temporal shift: on August 19 at the HIGH site (i.e. *CWTmax* had closest relationship with temperature averaged from August 9 to August 29,  $r = 0.378$ ), on September 1 at the MID site (from August 22 to September 11,  $r = 0.393$ ), and on September 15 at the LOW site (from September 5 to September 25,  $r = 0.291$ ).

There was no long-term instrumental observation of temperature at different elevations in the study area. Therefore, for analysis of dendroclimatic correlations, temperature series were corrected for each site according to their elevations and the average temperature lapse rate  $0.65^{\circ}\text{C}$  per 100 m (its verification is described in Online Resource 3). It should be noted that average temperature of maximum correlations' intervals was about  $9.5\text{-}9.6^{\circ}\text{C}$ , and at the end of these intervals it dropped to ca.  $7.7^{\circ}\text{C}$ .

Analysis of correlations of the *CWTmax* site chronologies with the dates of temperature drop below various threshold values as end-of-season indicators is presented in Online Resource 4. It showed the strongest response of *CWTmax* to the date of temperature crossing  $+9.5^{\circ}\text{C}$  threshold:  $r = 0.294$ ,  $0.340$ ,  $0.142$  at the HIGH, MID, and LOW sites respectively.

## 2.4 Spatiotemporal patterns in cell wall deposition and climatic variables important for it

As it was demonstrated in the previous research (Babushkina et al. 2019), spruces growing at the LOW and MID sites had similar *CWTmax* values ( $4.57 \pm 0.45$  and  $4.61 \pm 0.53$   $\mu\text{m}$ , difference is not significant at  $p < 0.05$ ), whereas at the HIGH site spruce tracheids had significantly thinner walls ( $3.37 \pm 0.34$   $\mu\text{m}$ ).

Correlation pattern of *CWTmax* was opposite: chronologies of the MID and HIGH sites were significantly correlated between each other ( $r = 0.54$ ) but not correlated at all with chronology of the LOW site ( $r = -0.01...0.02$ ).

In regards to long-term trends, the most substantial increase of *CWTmax* was observed at the MID site. It should be noted that it was not exactly linear at this elevation: increasing was more intensive in the 1960s–1980s, but almost stopped after achieving the same range of values as the ones observed at the lower limit of the spruce range (where mostly stable *CWTmax* decreased over the last decade). At the same time, increase of *CWTmax* was slower at the upper treeline than at the mid-range; statistical significance at  $p < 0.05$  was observed when comparing sub-periods' means, but not in the long-term linear trend. Time series of elevational differences between site chronologies of *CWTmax* tended to have more pronounced temporal trends and differences between the sub-periods (31–152% from values of the first sub-period) than site chronologies *per se*. The sum of cell wall area in the normalized radial file increased across all elevational distribution range of spruce; the difference in means between the sub-periods was by 6–7% at the two higher sites, whereas it was not statistically significant and was much lower (1.5%) at the LOW site. Wood density dynamics had even more pronounced elevational differences: increase by 5.5%, increase by 1.5%, and decrease by 6.5% at the HIGH, MID, and LOW sites respectively.

Dynamics of *CWTmax* is influenced by two climatic variables: the mean end-of-season temperature and the date of temperature crossing  $+9.5^{\circ}\text{C}$  threshold (Figure 5, Table 1). Due to the elevational temperature lapse, both these factors also have significant elevational shift: the period of maximum temperature impact on *CWTmax* occurs first at the HIGH site, than 13 days later at the MID site, and in 14 days earlier at the LOW site.; the date of temperature transition under  $+9.5^{\circ}\text{C}$  shifts between sites by 14–15 days. Long-term trends in both climatic factors had common pattern (warming and prolongation of growth season) across all transect, but were less pronounced at the LOW site in comparison with higher elevations, as was shown by both approaches (trends and differences in means). Unlike long-term trends, year-to-year dynamics of these variables was much less in sync between different elevations. Correlations of crucial temperatures were 0.20 between the LOW and HIGH sites, 0.44 between the LOW and MID sites, and 0.45 between the MID and HIGH sites; respective correlations of the threshold dates were 0.17, 0.39, and 0.46.

### 3 Discussion

We found that climate change impact on the spruce wood anatomical structure has common patterns for the study area as we hypothesized, but is also heavily modulated by elevational temperature gradient. It shows that in mountain forests of temperate continental zone, positive effect of warming on wood density increases from foothills to the treeline. Such observation may help us to better understand reaction of Siberian mountain forests to climate changes and its consequences regarding shift of annual carbon cycle.

#### 3.1 Spatiotemporal patterns in the local climate and their impact on spruce wood anatomy

The large and deep-water reservoir works as an accumulator of thermal energy due to the huge volume of water having high heat capacity. This leads to mitigation of the continental climate (a decrease in the amplitude of daily and seasonal temperature variation) and hysteresis, which is the delay of the local temperature dynamics compared with the regional one. This effect is aggravated by the fact that the dam in operation (i.e. when turbines are working) transmits water from the deep horizons of the reservoir, which is colder than at the surface in spring and summer, but warmer in autumn and winter. In winter, this leads to the formation of a non-freezing polynya extending up to hundred kilometers downstream from the dam, additionally warming the local climate (Kosmakov 2001). Probably because of this, the sharpest jump in winter temperatures coincided with the launch of the first hydroelectric turbines. The beginning of the reservoir impact on climate in 1980 was confirmed not only by this jump in the difference series, but also by higher correlations of local and regional temperatures of the cold season during two separate sub-periods (before and after 1980) compared to the entire period of instrumental observations.

The combination of the aforementioned effects led to the fact that summer temperatures were stable, whereas duration of the growth season, spring and autumn temperatures increased (more in autumn than

in spring). At the upper treeline, an increase in heat supply was observed only at the very beginning and end of the growth season (since this season itself is short and most of its length accounts for the interval of stable temperatures), yielding the prevalence of seasonality change in regards to the dynamics of growth–climate relationship. As the elevation descends to the dam, the growth season extends to time intervals characterized by more substantial warming, leading also to the significant heat supply increase.

Due to the elevational shift of *CWT<sub>max</sub>* formation to the earlier dates from foothills to the alpine zone, the 21-day series of temperature crucial for *CWT<sub>max</sub>* overlap only for 7–8 days between closer sites and do not overlap at all between the LOW and HIGH sites, which leads to a drop of correlations between these climatic variables (cf. inter-annual fluctuations of crucial temperature in [Figure 5c](#)). Still significant positive correlations between the LOW and HIGH sites can be attributed to the common warming trend. This spatiotemporal shift in temperature series is also at least partially responsible for the low correlations between the site chronologies of *CWT<sub>max</sub>*, as they register temperature fluctuations of different time intervals during season.

At the upper limit of spruce growth, *CWT* and *CWA* increase after transition to latewood less considerably than at the lower elevations. The most likely cause of this phenomenon is low heat supply during the entire growth season, limiting the rates of growth processes, including cell wall deposition. An argument in favor of this assumption is that the size of the tracheids, which is formed as a result of the less resource-intensive process of cell expansion ([Cuny et al. 2015](#)), suffers from temperature lapse to a lesser extent. On the other hand, the absence of significant differences in *CWT* and *CWA* between the MID and LOW sites indirectly indicates that the secondary wall deposition in the lower part of the spruce range reaches its limits due to internal restrictions (genetically predetermined wood structure providing trade-offs between efficiency and safety of water conduction, between structural strength and carbon cost; geometrical limitation of wall deposition by cell size  $CWT < D/2$ , etc.).

The local climate change by the reservoir dam, as well as increase of tree age and size with time (leading to increase of cell/lumen size and mean *CWT* from pith to bark and from top to bottom, see [Anfodillo et al 2006](#); [Lachenbruch et al 2011](#); [Carrer et al 2015](#); [Rosell et al 2017](#)), led to certain shifts in the wood anatomical structure, having both a common component for all elevational range of spruce distribution. It is difficult to distinguish between these two reasons of long-term variation in wood anatomy, because age- or size-related trends are close to linear beyond juvenile wood (first 5–20 tree rings from pith, [Zobel and Sprague 1998](#)). Moreover, meta-analysis of wood hydraulic architecture ([Mencuccini et al. 2007](#)) showed that unlike angiosperms, large conifer trees increase their tracheids downward only in higher part of tree, and have relatively constant tracheid size in lower part of trunk. It means that the same constant trend in mature wood may be valid for radial pattern of wood anatomical parameters. Further research of age/size patterns in spruce xylem architecture for the study area seems to be of interest, but it requires additional anatomical measurements including trees of various ages during period before current warming.

At the upper treeline, an increase was observed in the results of both processes of the tracheids expansion and the secondary wall deposition. The presence of this reaction in earlywood may indicate a positive role not only of the later ending of the growth season, but also of its earlier onset. However, even under the changed conditions, *CWA* is not much higher in latewood than in earlywood at the HIGH site, due to the strong limitation of the rate of cell wall deposition by temperature. The positive effect of warming on *D* is increasing down the entire transect, while the process of wall deposition is stimulated by warming only up to a certain limit, apparently internal: physiological (preservation of the water transport efficiency) or genetic. However, since a greater amount of deposited wood matter is distributed over the larger cell perimeter, this leads to the fact that *CWT* increases to a lesser extent than *CWA*. As a result, a significant elevational gradient is observed in the impact of warming on wood density. Thus, both the switch of the main growth-limiting factor due to the climatic gradients in mountains and the internal limitations of the tracheid parameters' values are reflected in the anatomical structure of wood and its dynamics along the elevational transect.

### **3.2 Role of temperature in the regulation of wood matter deposition in tracheids**

The onset of growth processes for spruce in the study area is determined by the temperature threshold,

since even at the lower limit of growth, where moisture availability is minimal, the arrangement of the spruce trees along the stream prevents this phenological event from being delayed by lack of moisture, which is often observed in semiarid regions (Ren et al. 2015, 2018; Ziaco et al. 2018). At the same time, wood formation phenology of spruce is also regulated by other factors. E.g., , for conifers in temperate and cold climates, close linear relationships were found both between the timing of the onset of successive tracheid differentiation stages and between their durations (Rossi et al. 2013). Given the relatively constant photoperiod-regulated date of cambial activity cessation, the earlier start of the growth season leads to an increase in the duration of cambial activity, and hence durations of the subsequent stages. However, at the end of the season, wood development cessation and dormancy can be regulated in two ways: (1) “emergency”, when the temperature drops below the critical threshold, or (2) “regular” growth cessation due to a decrease in the photoperiod length and the natural chain of completion of growth processes, which is regulated internally by dynamics of hormone concentration and gene expression (cf. Rossi et al. 2009; Tanino et al. 2010; Cooke et al. 2012); hence the relationships observed by Rossi et al. (2013) are weaker at the end of the season. Obviously, the shorter the warm season, the greater the likelihood of triggering “emergency” growth cessation, which leads to the formation of relatively thin-walled latewood cells (the so-called light rings; Filion et al. 1986). This is consistent with our observations of *CWA* and *CWT* reaction to the end-of-season temperatures/dates and the form of their tracheidograms not only at the upper treeline throughout the whole period under consideration, but also to some extent at the MID site, particularly before warming. In the lower part of the spruce range, the growth season duration is usually sufficient for the “regular” completion of the tree ring formation, which leads to a decrease in the cell wall parameters’ response to temperature and especially to the date of its transition below the crucial threshold. It should be noted that the threshold value of  $+9.5^{\circ}\text{C}$  obtained in this study indicate rather the temperature at which the growth processes begin to be inhibited (since it is the average temperature for the whole crucial 21-day period), whereas the full growth cessation is most likely to occur at ca.  $+7.7^{\circ}\text{C}$  observed at the end of this period (Table S3 in Online Resource 3), which converges with generalized estimation of temperature threshold  $+6\text{--}8^{\circ}\text{C}$  for xylogenesis obtained by Rossi et al. (2008) for a wide range of conifer species and growth conditions. It would be of interest in the further research to verify these guesses with direct observations of the tree-ring formation seasonal kinetics in the same sampling sites.

It is interesting, that *CWT*<sub>max</sub> at the LOW site is almost independent of the end-of-season timing, but still has a significant response to the temperature in September. Possible reason is direct positive influence of of heat supply throughout the season (regardless of its duration) on growth, including the rate of wood matter deposition in cell walls. An indirect confirmation of this assumption is the increase in both *D* and *CWA* with climate warming at all elevations, as well as the corresponding elevational gradients in the average values of anatomical parameters and radial growth (Babushkina et al. 2018a, 2019).

As previously identified, spruce stands as a whole in the study area are characterized by the absence of sharp growth depressions en masse and the presence of spruce saplings and young trees, both under the impact of only regional climate trend and after local warming of the climate (Babushkina et al. 2018a), which makes them stable carbon sink. However, this study showed that the dynamics of carbon fixation, recorded in cell production, is complicated by the impact of climate change on the later stages of xylem differentiation, primarily on the deposition of the secondary cell wall. Growth intensification at this stage leads to the formation of more dense wood, “packing” more carbon in the same volume or cross-sectional area. Therefore, based on radial growth estimations of biomass increment and carbon sequestration in forest can be refined by taking into account variation of wood density (Cuny et al. 2015). In our case, on the scale of one measured radial file of cells in one ring, warming-induced increase in the area of wood matter seems scanty:  $60\text{--}260\ \mu\text{m}^2$  on the average (i.e. for tree ring of mean width at respective site); however, when scaling to full basal area increment (BAI) of tree, the total additional area is already  $0.08\text{--}0.18\ \text{cm}^2$  on the average, and for local stands the additional deposition of wood matter just by spruce (comprising  $10\text{--}30\%$  of mixed forest stand) can be roughly estimated at average  $1650\text{--}7100\ \text{cm}^3/\text{ha}$  per year (Online Resource 5).

It was recently shown that during the last decades, despite later ending of the warm season due to global warming, carbon dioxide build-up in autumn has shifted to earlier dates (Piao et al. 2008). Findings of this study let us suggest that such a discrepancy may be caused by the predominance (in covered area and net productivity) of forests that are characterized by the photoperiod-regulated growth cessation of prevailing tree species/provenances acclimated to conditions of long warm season . In their case, warming



in autumn is not accompanied by phenological shifts and an increase in carbon deposition in the xylem, but stimulates respiration (carbon loss), reducing the contribution of such a forest to carbon sequestration. On the other hand, for cold boreal and high mountain forests, effect of autumn carbon loss should not occur as long as end-of-season temperature crosses crucial threshold for growth earlier than the natural completion of growth, increasing their role in the global carbon balance of a rapidly warming world.

## 4 Conclusion

The revealed regularities and elevational gradients in the anatomical structure of wood and its response to local warming showed that an earlier start of the growth season leads to an increase of both tracheid radial size and cell wall thickness. At the same time, increasing temperatures at the end of the growth season prolongs its duration and increases carbon deposition in the most thick-walled cells of latewood only to a certain limit. The possible reason may be switch of spruce growth cessation to the mechanism of regulation by photoperiod and internally-determined duration of the tracheid differentiation stages if warm season is long enough. Taking into account direct regulation of the growth rates by heat supply, its increase in the second half of the season leads to an increase in deposition of woody matter in the walls of tracheids, significantly more pronounced for the upper part of the spruce distribution range, where tree ring formation is limited by the duration of the warm season.

## References

- Anfodillo T, Carraro V, Carrer M, et al. (2006) Convergent tapering of xylem conduits in different woody species. *New Phytologist* 169(2): 279–290. <https://doi.org/10.1111/j.1469-8137.2005.01587.x>
- Arzac A, Babushkina EA, Fonti P, et al. (2018) Evidences of wider latewood in *Pinus sylvestris* from a forest-steppe of Southern Siberia. *Dendrochronologia* 49: 1–8. <https://doi.org/10.1016/j.dendro.2018.02.007>
- Babushkina E, Belokopytova L, Zhirnova D, et al. (2018a) Divergent growth trends and climatic response of *Picea obovata* along elevational gradient in Western Sayan mountains, Siberia. *Journal of Mountain Science* 15(11): 2378–2397. <https://doi.org/10.1007/s11629-018-4974-6>
- Babushkina EA, Belokopytova LV, Zhirnova DF, et al. (2018b) Climatically driven yield variability of major crops in Khakassia (South Siberia). *International Journal of Biometeorology* 62(6): 939–948. <https://doi.org/10.1007/s00484-017-1496-9>
- Babushkina EA, Belokopytova LV, Zhirnova DF, Vaganov EA (2019) Siberian spruce tree ring anatomy: imprint of development processes and their high-temporal environmental regulation. *Dendrochronologia* 53: 114–124. <https://doi.org/10.1016/j.dendro.2018.12.003>
- Badeck FW, Bondeau A, Bottcher K, et al. 2004. Responses of spring phenology to climate change. *New Phytologist* 162: 295–309. <http://doi:10.1111/j.1469-8137.2004.01059.x>
- Belokopytova LV, Babushkina EA, Zhirnova DF, et al. (2018) Climatic response of conifer radial growth in forest-steppes of South Siberia: comparison of three approaches. *Contemporary Problems of Ecology* 11(4): 366–376. <https://doi.org/10.1134/S1995425518040030>
- Belokopytova LV, Babushkina EA, Zhirnova DF, et al. (2019) Pine and larch tracheids capture seasonal variations of climatic signal at moisture-limited sites. *Trees* 33(1): 227–242. <https://doi.org/10.1007/s00468-018-1772-2>
- Case BS, Duncan RP (2014) A novel framework for disentangling the scale-dependent influences of abiotic factors on alpine treeline position. *Ecography* 37(9): 838–851. <https://doi.org/10.1111/ecog.00280>
- Carrer M, von Arx G, Castagneri D, Petit G (2015) Distilling allometric and environmental information from time series of conduit size: the standardization issue and its relationship to tree hydraulic architecture. *Tree Physiology* 35(1): 27–33. <https://doi.org/10.1093/treephys/tpu108>
- Carrer M, Castagneri D, Prendin AL, Petit G, von Arx G (2017) Retrospective analysis of wood anatomical traits reveals a recent extension in tree cambial activity in two high-elevation conifers. *Frontiers in Plant Science* 8: 737. <https://doi.org/10.3389/fpls.2017.00737>
- Castagneri D, Battipaglia G, von Arx G, et al. (2018) Tree-ring anatomy and carbon isotope ratio show both direct and legacy effects of climate on bimodal xylem formation in *Pinus pinea*. *Tree Physiology* 38(8): 1098–1109. <https://doi.org/10.1093/treephys/tpy036>
- Chae H, Lee H, Lee S, et al. (2012) Local variability in temperature, humidity and radiation in the Baekdu Daegan Mountain protected area of Korea. *Journal of Mountain Science* 9(5): 613–627. <https://doi.org/10.1007/s11629-012-2347-0>
- Chave J, Coomes D, Jansen S, et al. (2009) Towards a worldwide wood economics spectrum. *Ecology Letters* 12(4): 351–366. <https://doi.org/10.1111/j.1461-0248.2009.01285.x>
- Christidis N, Stott PA, Brown S, et al. (2007) Human contribution to the lengthening of the growing season during 1950–99. *Journal of Climate* 20(21): 5441–5454. <https://doi.org/10.1175/2007JCLI1568.1>
- Churkina G, Schimel, D, Braswell BH, Xiao X (2005) Spatial analysis of growing season length control over net ecosystem exchange. *Global Change Biology* 11(10): 1777–1787. <https://doi.org/10.1111/j.1365-2486.2005.001012.x>
- Cook ER, Kairiukstis LA (eds.) (1990) *Methods of Dendrochronology. Application in Environmental Sciences*. Dordrecht, Boston, London: Kluwer Academic Publishers. p 394.
- Cooke JE, Eriksson ME, Junntila O (2012) The dynamic nature of bud dormancy in trees: environmental control and molecular mechanisms. *Plant, Cell & Environment* 35(10): 1707–1728. <https://doi.org/10.1111/j.1365-3040.2012.02552.x>
- Cuny HE, Rathgeber CB, Frank D, et al. (2015) Woody biomass production lags stem-girth increase by over one month in coniferous forests. *Nature Plants* 1(11): 15160. <https://doi.org/10.1038/nplants.2015.160>
- Davi H, Dufréne E, Francois C, et al. (2006) Sensitivity of water and carbon fluxes to climate changes from 1960 to 2100 in European forest ecosystems. *Agricultural and Forest Meteorology* 141(1): 35–56. <https://doi.org/10.1016/j.agrformet.2006.09.003>

- Demina AV, Belokopytova LV, Andreev SG, et al. (2017) Radial increment dynamics of Scots pine (*Pinus sylvestris* L.) as an indicator of hydrothermal regime of the Western Transbaikalia forest steppe. *Contemporary Problems of Ecology* 10(5): 476–487. <https://doi.org/10.1134/S1995425517050031>
- Deslauriers A., Fonti P., Rossi S., et al. (2017) Ecophysiology and plasticity of wood and phloem formation. In: Amoroso M. et al. (eds.), *Dendroecology. Tree-Ring Analyses Applied to Ecological Studies*. Springer, Cham. pp 13–33. [https://doi.org/10.1007/978-3-319-61669-8\\_2](https://doi.org/10.1007/978-3-319-61669-8_2)
- Eilmann B, Zweifel R, Buchmann N, et al. (2009) Drought-induced adaptation of the xylem in Scots pine and pubescent oak. *Tree Physiology* 29(8): 1011–1020. <https://doi.org/10.1093/treephys/tpp035>
- Filion L, Payette S, Gauthier L, Boutin Y (1986) Light rings in subarctic conifers as a dendrochronological tool. *Quaternary Research* 26(2): 272–279. [https://doi.org/10.1016/0033-5894\(86\)90111-0](https://doi.org/10.1016/0033-5894(86)90111-0)
- Fonti P, von Arx G, García-González I, et al. (2010) Studying global change through investigation of the plastic responses of xylem anatomy in tree rings. *New Phytologist* 185(1): 42–53. <https://doi.org/10.1111/j.1469-8137.2009.03030.x>
- Frich P, Alexander LV, Della-Marta PM, et al. (2002) Observed coherent changes in climatic extremes during the second half of the twentieth century. *Climate Research* 19(3): 193–212. <https://doi.org/10.3354/cro19193>
- Fritts HC (1976) *Tree Rings and Climate*. London: Academic Press. p 582.
- Fritts HC, Swetnam TW (1989) *Dendroecology: a tool for evaluating variations in past and present forest environments*. *Advances in Ecological Research* 19: 111–188. [https://doi.org/10.1016/S0065-2504\(08\)60158-0](https://doi.org/10.1016/S0065-2504(08)60158-0)
- Gričar J, Prislán P, de Luis M, et al. (2015) Plasticity in variation of xylem and phloem cell characteristics of Norway spruce under different local conditions. *Frontiers in Plant Science* 6: 730. <https://doi.org/10.3389/fpls.2015.00730>
- Hamlet AF, Lettenmaier DP (2005) Production of temporally consistent gridded precipitation and temperature fields for the continental United States. *Journal of Hydrometeorology* 6(3): 330–336. <https://doi.org/10.1175/JHM420.1>
- Hänninen H, Tanino K (2011) Tree seasonality in a warming climate. *Trends in Plant Science* 16(8): 412–416. <https://doi.org/10.1016/j.tplants.2011.05.001>
- Keeling CD, Chin JFS, Whorf TP (1996) Increased activity of northern vegetation inferred from atmospheric CO<sub>2</sub> measurements. *Nature* 382: 146–149. <https://doi.org/10.1038/382146a0>
- Keenan TF, Gray J, Friedl MA, et al. (2014) Net carbon uptake has increased through warming-induced changes in temperate forest phenology. *Nature Climate Change*, 4(7): 598. <https://doi.org/10.1038/NCLIMATE2253>
- Kilpeläinen A, Peltola H, Ryyppö A, et al. (2003) Wood properties of Scots pines (*Pinus sylvestris*) grown at elevated temperature and carbon dioxide concentration. *Tree Physiology* 23(13): 889–897. <https://doi.org/10.1093/treephys/23.13.889>
- Körner C, Basier D (2010) Phenology under global warming. *Science* 327(5972): 1461–1462. <https://doi.org/10.1126/science.1186473>
- Kosmakov IV (2001) Thermal and Ice Regime in the Upper and Lower Reaches of High-Pressure Hydroelectric Power Stations on the Yenisei. *Krasnoyarsk: Klaretianum*. p 142. (In Russian)
- Lachenbruch B, Moore JR, Evans R. (2011) Radial variation in wood structure and function in woody plants, and hypotheses for its occurrence. In: Meinzer FC et al. (eds.) *Size- and Age-Related Changes in Tree Structure and Function*. Dordrecht: Springer, pp. 121–164. [https://doi.org/10.1007/978-94-007-1242-3\\_5](https://doi.org/10.1007/978-94-007-1242-3_5)
- Larson PR (1994) *The Vascular Cambium. Development and Structure*. Berlin, Heidelberg: Springer-Verlag. p 725.
- Lei H, Milota MR, Gartner BL (1996) Between- and within-tree variation in the anatomy and specific gravity of wood in Oregon white oak (*Quercus garryana* Dougl.). *IAWA Journal* 17(4): 445–461. <https://doi.org/10.1163/22941932-90000642>
- Leuzinger S, Luo Y, Beier C, et al. (2011) Do global change experiments overestimate impacts on terrestrial ecosystems?. *Trends in Ecology & Evolution* 26(5): 236–241. <https://doi.org/10.1016/j.tree.2011.02.011>
- Ma Q, Huang JG, Hänninen H, Berninger F (2018) Reduced geographical variability in spring phenology of temperate trees with recent warming. *Agricultural and Forest Meteorology* 256: 526–533. <https://doi.org/10.1016/j.agrformet.2018.04.012>
- Malanson GP (2017) Mixed signals in trends of variance in high-elevation tree ring chronologies. *Journal of Mountain Science* 14(10): 1961–1968. <https://doi.org/10.1007/s11629-017-4425-9>
- Maurer EP, Wood AW, Adam JC, et al. (2002) A long-term hydrologically based dataset of land surface fluxes and states for the conterminous United States. *Journal of Climate* 15(22): 3237–3251. [https://doi.org/10.1175/1520-0442\(2002\)015<3237:ALTHBD>2.0.CO;2](https://doi.org/10.1175/1520-0442(2002)015<3237:ALTHBD>2.0.CO;2)
- Mencuccini M, Hölttä T, Petit G, Magnani F (2007) Sanio's laws revisited. Size- dependent changes in the xylem architecture of trees. *Ecology Letters* 10(11):1084–1093. <https://doi.org/10.1111/j.1461-0248.2007.01104.x>
- Menzel A (2000). Trends in phenological phases in Europe between 1951 and 1996. *International Journal of Biometeorology*, 44(2): 76–81. <https://doi.org/10.1007/s004840000054>
- Panyushkina IP, Hughes MK, Vaganov EA, Munro MA (2003) Summer temperature in northeastern Siberia since 1642 reconstructed from tracheid dimensions and cell numbers of *Larix cajanderi*. *Canadian Journal of Forest Research* 33(10): 1905–1914. <https://doi.org/10.1139/x03-109>
- Pedlar JH, McKenney DW, Lawrence K, et al. (2015) A comparison of two approaches for generating spatial models of growing-season variables for Canada. *Journal of Applied Meteorology and Climatology* 54(2): 506–518. <https://doi.org/10.1175/JAMC-D-14-0045.1>
- Peltola H, Kilpeläinen A, Kellomäki S (2002) Diameter growth of Scots pine (*Pinus sylvestris*) trees grown at elevated temperature and carbon dioxide concentration under boreal conditions. *Tree Physiology* 22(14): 963–972. <https://doi.org/10.1093/treephys/22.14.963>
- Peñuelas J, Filella I (2009) Phenology feedbacks on climate change. *Science* 324(5929): 887–888. <https://doi.org/10.1126/science.1173004>
- Piao S, Ciais P, Friedlingstein P al. (2008) Net carbon dioxide losses of northern ecosystems in response to autumn warming. *Nature* 451(7174): 49–52. <https://doi.org/10.1038/nature06444>
- Polikarpov NP, Nazimova DI (1963) The dark coniferous forests of the northern part of the west Siberian mountains. In: *Forestry Research in the Forests of Siberia*. Krasnoyarsk: Institute for Forests and Wood. Vol. 57. pp. 103–147. (In Russian).
- Plomion C, Leprovost G, Stokes A (2001) Wood formation in trees. *Plant Physiology* 127(4): 1513–1523. <https://doi.org/10.1104/pp.010816>
- Popov AV, Shatravskii AI (1994) Removal of floating timber from the Sayano-Shushenskoe hydrostation reservoir. *Hydrotechnical Construction* 28(4): 204–208. <https://doi.org/10.1007/BF01545054>
- Price MF, Byers AC, Friend DA, et al. (eds.) (2013) *Mountain Geography: Physical and Human Dimensions*. Berkeley: University of California Press. p 378.
- Ren P, Rossi S, Gričar J, et al. (2015) Is precipitation a trigger for the onset of xylogenesis in *Juniperus przewalskii* on the north-eastern Tibetan Plateau? *Annals of Botany* 115(4): 629–639. <https://doi.org/10.1093/aob/mcu259>
- Ren P, Rossi S, Camarero JJ, et al. (2018) Critical temperature and precipitation thresholds for the onset of xylogenesis of *Juniperus przewalskii* in a semi-arid area of the north-eastern Tibetan Plateau. *Annals of Botany* 121(4): 617–624. <https://doi.org/10.1093/aob/mcx188>

- Root TL, Price JT, Hall KR, et al. (2003) Fingerprints of global warming on wild animals and plants. *Nature* 421: 57–60. <https://doi.org/10.1038/nature01333>
- Rosell JA, Olson ME, Anfodillo T (2017) Scaling of xylem vessel diameter with plant size: causes, predictions, and outstanding questions. *Current Forestry Reports* 3(1): 46–59. <https://doi.org/10.1007/s40725-017-0049-0>
- Rosgidromet (2010) Guidelines for the Compilation of Agrometeorological Yearbook for the Agricultural Zone of the Russian Federation (Guiding Document 52.33.725-2010). Obninsk: Russian Scientific Research Institute of Hydrometeorological Information, World Data Center. p 142. (In Russian)
- Rossi S, Deslauriers A, Gričar J, et al. (2008) Critical temperatures for xylogenesis in conifers of cold climates. *Global Ecology and Biogeography* 17(6): 696–707. <https://doi.org/10.1111/j.1466-8238.2008.00417.x>
- Rossi S, Rathgeber CB, Deslauriers A (2009) Comparing needle and shoot phenology with xylem development on three conifer species in Italy. *Annals of Forest Science* 66(2): 1–8. <https://doi.org/10.1051/forest/2008088>
- Rossi S, Anfodillo T, Čufar K, et al. (2013) A meta-analysis of cambium phenology and growth: linear and non-linear patterns in conifers of the northern hemisphere. *Annals of Botany* 112(9): 1911–1920. <https://doi.org/10.1093/aob/mct243>
- Schickhoff U, Bobrowski M, Böhner J, et al. (2015) Do Himalayan treelines respond to recent climate change? An evaluation of sensitivity indicators. *Earth System Dynamics* 6: 245–265. <https://doi.org/10.5194/esd-6-245-2015>
- Schweingruber FH (1988) *Tree Rings: Basics and Applications of Dendrochronology*. Dordrecht: Springer. p 276. <https://doi.org/10.1007/978-94-009-1273-1>
- Schweingruber FH (2006) Anatomical characteristics and ecological trends in the xylem and phloem of Brassicaceae and Resedaceae. *Iawa Journal* 27(4): 419–442. <https://doi.org/10.1163/22941932-90000164>
- Seo JW, Smiljanić M, Wilmking M (2014) Optimizing cell-anatomical chronologies of Scots pine by stepwise increasing the number of radial tracheid rows included – Case study based on three Scandinavian sites. *Dendrochronologia* 32(3): 205–209. <https://doi.org/10.1016/j.dendro.2014.02.002>
- Silkin PP (2010) *Methods of Multiparameter Analysis of Conifers Tree-Rings Structure*. Krasnoyarsk: Siberian Federal University. p 335. (In Russian)
- Skomarkova MV, Vaganov EA, Mund M, et al. (2006) Inter-annual and seasonal variability of radial growth, wood density and carbon isotope ratios in tree rings of beech (*Fagus sylvatica*) growing in Germany and Italy. *Trees* 20(5): 571–586. <https://doi.org/10.1007/s00468-006-0072-4>
- Stamm AJ (1929) Density of wood substance, adsorption by wood, and permeability of wood. *The Journal of Physical Chemistry* 33(3): 398–414.
- Stinziano JR, Way DA (2014) Combined effects of rising [CO<sub>2</sub>] and temperature on boreal forests: growth, physiology and limitations. *Botany* 92(6): 425–436. <https://doi.org/10.1139/cjb-2013-0314>
- Taeger S, Sparks TH, Menzel A (2015) Effects of temperature and drought manipulations on seedlings of Scots pine provenances. *Plant Biology* 17(2): 361–372. <https://doi.org/10.1111/plb.12245>
- Tanino KK, Kalcsits L, Silim S, et al. (2010) Temperature-driven plasticity in growth cessation and dormancy development in deciduous woody plants: a working hypothesis suggesting how molecular and cellular function is affected by temperature during dormancy induction. *Plant Molecular Biology* 73(1–2): 49–65. <https://doi.org/10.1007/s11103-010-9610-y>
- Vaganov EA, Shashkin AV, Sviderskaya LV, Vysotskaya LG (1985) *Histometric Analysis of Woody Plant Growth*. Novosibirsk: Nauka. p 102. (In Russian)
- Vaganov EA, Hughes MK, Shashkin AV (2006) *Growth Dynamics of Conifer Tree Rings: Images of Past and Future Environments*. Berlin, Heidelberg: Springer-Verlag. p 358.
- Vysotskaya LG, Vaganov EA (1989) Components of the variability of radial cell size in tree rings of conifers. *IAWA Journal* 10(4): 417–426. <https://doi.org/10.1163/22941932-90001134>
- Wang X, Gao Q, Wang C, Yu M (2017) Spatiotemporal patterns of vegetation phenology change and relationships with climate in the two transects of East China. *Global Ecology and Conservation* 10: 206–219. <https://doi.org/10.1016/j.gecco.2017.01.010>
- Wieser G, Holtmeier FK, Smith WK (2014) Treelines in a changing global environment. In: Tausz M, Grulke N (eds.), *Trees in a Changing Environment*. Springer, Dordrecht, The Netherlands. pp 221–263. <https://doi.org/10.1007/978-94-017-9100-7>
- Wolkovich EM, Cook BI, Allen JM, et al. (2012) Warming experiments under predict plant phenological responses to climate change. *Nature* 485: 494–497. <https://doi.org/10.1038/nature11014>
- Wypych A, Ustrnul Z, Schmatz DR (2018) Long-term variability of air temperature and precipitation conditions in the Polish Carpathians. *Journal of Mountain Science* 15(2): 237–253. <https://doi.org/10.1007/s11629-017-4374-3>
- Ziaco E, Biondi F (2016) Tree growth, cambial phenology, and wood anatomy of limber pine at a Great Basin (USA) mountain observatory. *Trees* 30(5): 1507–1521. <https://doi.org/10.1007/s00468-016-1384-7>
- Ziaco E, Truettner C, Biondi F, Bullock S (2018) Moisture-driven xylogenesis in *Pinus ponderosa* from a Mojave Desert mountain reveals high phenological plasticity. *Plant, Cell & Environment* 41(4): 823–836. <https://doi.org/10.1111/pce.13152>
- Zobel BJ, Sprague JR (1998) *Juvenile Wood in Forest Trees*. Berlin: Springer. p 300.

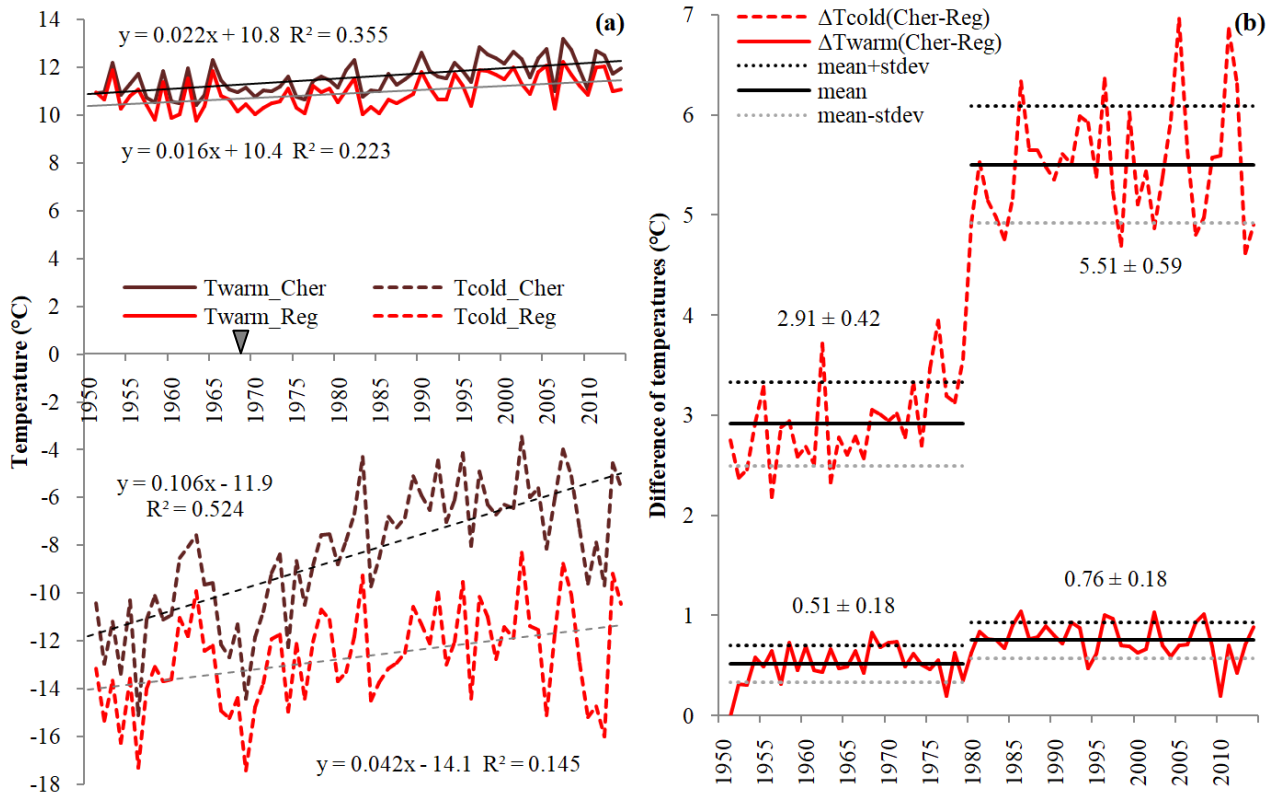


**Figure 1** Regional (Reg) and local (Cher) climatic dynamics: (a) trends of the warm (April–October) and the cold (November–March) season average temperature; all trends are significant at the level  $p < 0.05$ ; (b) difference series for local and regional average temperature during the same seasons; its *mean*  $\pm$  *stdev* values are presented for 1951–1979 and 1980–2014 sub-periods. On the horizontal axes, year of dam building beginning (1968, grey triangle), periods of reservoir filling (1975–1990, blue bar) and turbines launching (from the end of 1979 to the end of 1985, yellow bar) are shown; the most pronounced temperature shifts occurred after the first turbines' launching

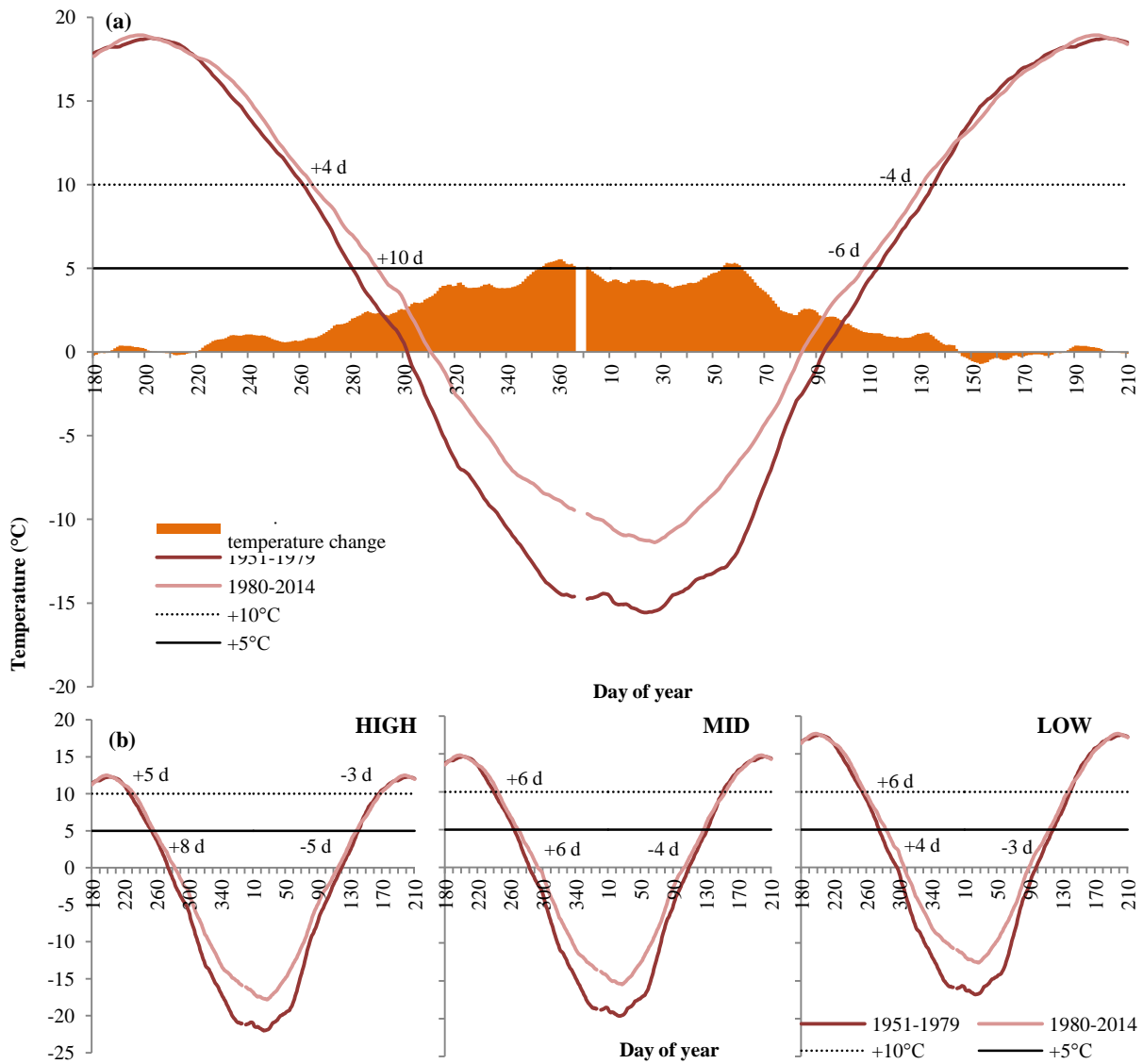


**Figure 2** Intra-annual local temperature dynamics before and since 1980: (a) daily temperatures at the Cheryomushki station smoothed by 21-day moving average and then averaged for the whole sub-periods; (b) the same, but at the elevations of sampling sites, accounting temperature lapse rate as 0.65°C per 100 m. According to Rossi et al. (2008), temperature threshold for xylogenesis of conifers usually ranges between +5°C and +10°C, these values are marked on all plots

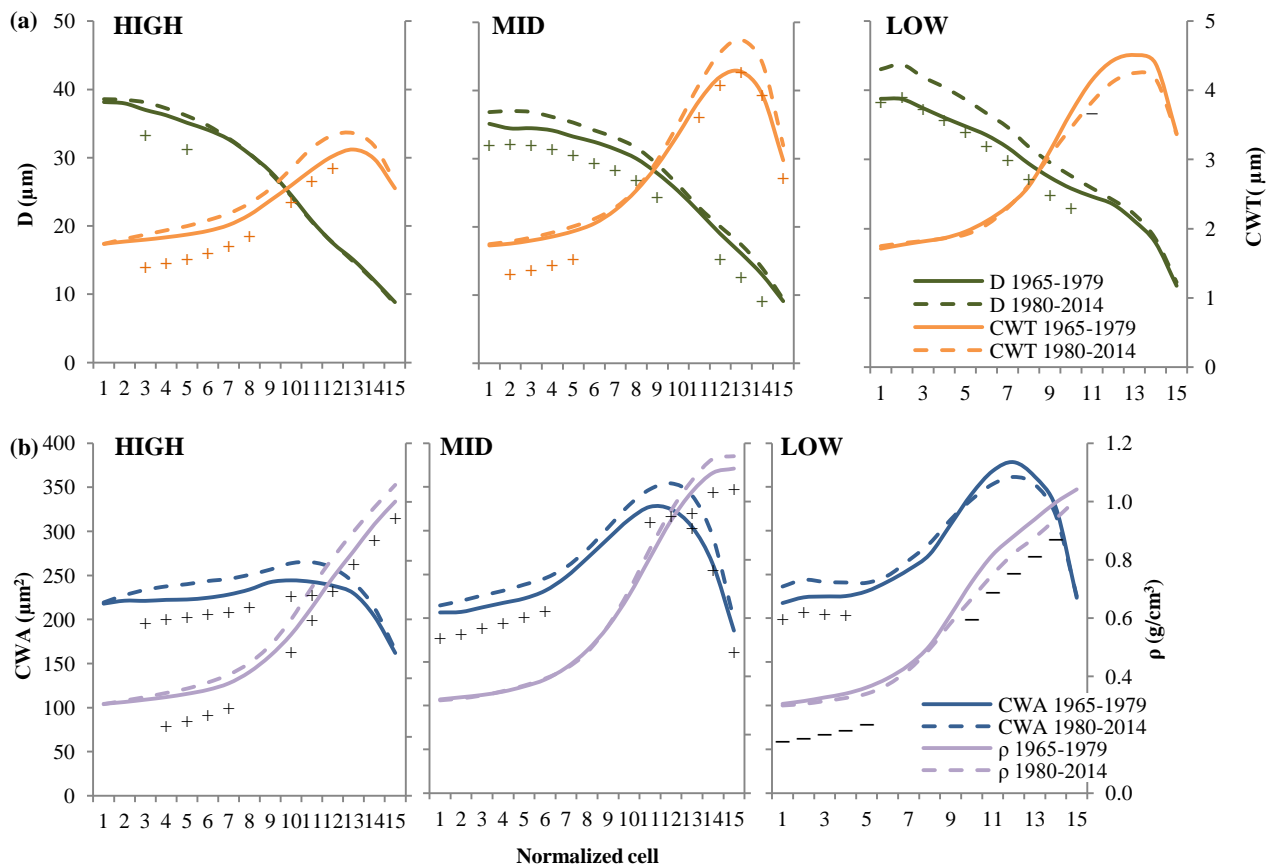


**Figure 3** Normalized tracheidograms averaged for 1965-1979 and 1980-2014 sub-periods: (a) basic traits – tracheid radial diameter  $D$  and cell wall thickness  $CWT$ ; (b) derivative traits – cell wall area  $CWA$  and wood density  $\rho$ . Significant at the level  $p < 0.05$  differences in means between the sub-periods are marked with “+” and “-” signs according to directions of change

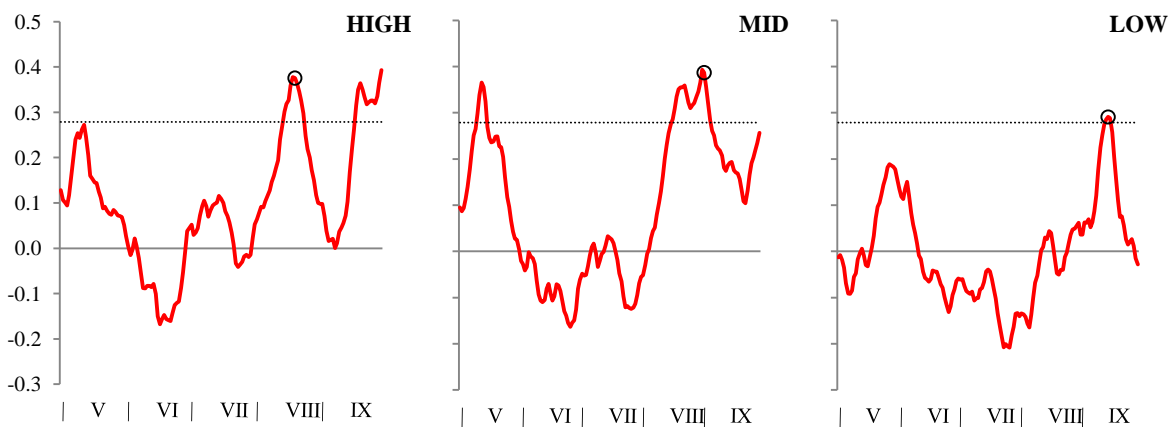


**Figure 4** Correlations between  $CWT_{max}$  site chronologies and 21-day moving temperature series from May to September. Markers represent maximum correlations. Dot lines mark the correlation significance level  $p = 0.05$

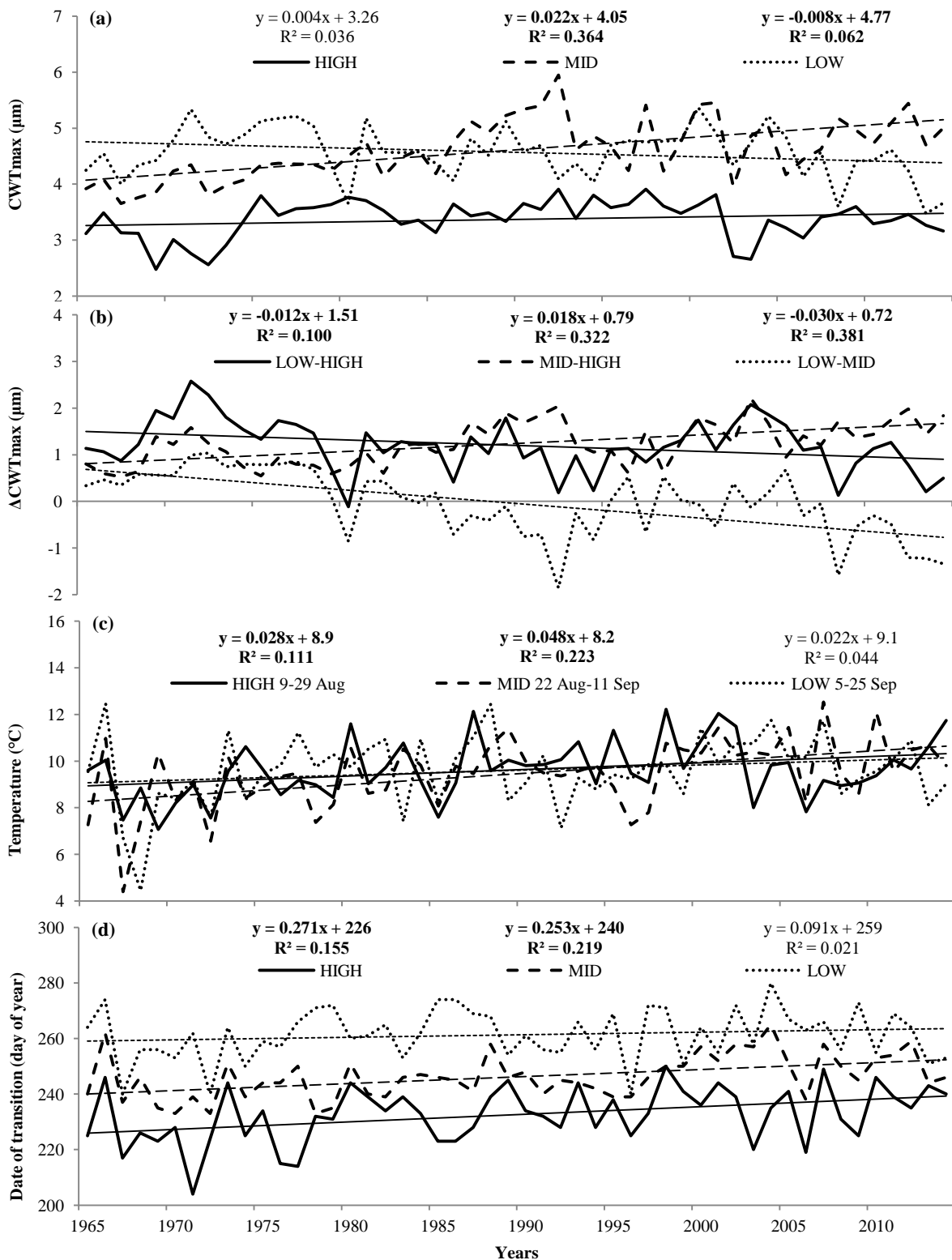


**Figure 5** Long-term linear trends in the *CWTmax* site chronologies and climatic variables important for its formation: (a) site chronologies of *CWTmax*; (b) differences between them; (c) mean temperature during crucial 21-day period ([Online Resource 2](#)); (d) date of the temperature crossing +9.5°C threshold. Equations of trends significant at the level  $p < 0.05$  are written in bold

**Table 1** Spruce anatomical parameters and climatic variables (*mean ± stdev*) over sub-periods before and since 1980 and over all period of anatomical measurements

Site	Period			Difference between sub-periods	
	1965-2014	1965-1979	1980-2014	value	significance level, <i>p</i>
Site chronologies of <i>CWTmax</i> (μm)					
HIGH	3.37 ± 0.34	3.20 ± 0.40	3.45 ± 0.29	<b>+0.25(7.9%)</b>	<b>0.039</b>
MID	4.61 ± 0.53	4.09 ± 0.25	4.84 ± 0.46	<b>+0.75(18.2%)</b>	<b>&lt;0.001</b>
LOW	4.57 ± 0.45	4.73 ± 0.40	4.50 ± 0.46	-0.23(-4.9%)	0.082
Time series of difference between site chronologies of <i>CWTmax</i> (μm)					
LOW-HIGH	1.20 ± 0.56	1.54 ± 0.51	1.05 ± 0.52	<b>-0.49(-31.5%)</b>	<b>0.005</b>
MID-HIGH	1.24 ± 0.45	0.90 ± 0.33	1.39 ± 0.42	<b>+0.49(55.0%)</b>	<b>&lt;0.001</b>
LOW-MID	-0.04 ± 0.70	0.64 ± 0.26	-0.33 ± 0.62	<b>-0.97(-152.0%)</b>	<b>&lt;0.001</b>
Total cell wall area, $\Sigma CWA$ (μm <sup>2</sup> )					
HIGH	3500 ± 240	3360 ± 310	3560 ± 180	<b>+200(6.2%)</b>	<b>0.026</b>
MID	4000 ± 270	3820 ± 220	4080 ± 250	<b>+260(6.8%)</b>	<b>0.001</b>
LOW	4240 ± 360	4200 ± 450	4260 ± 320	+60(1.5%)	0.625
Mean wood density, $\rho_{mean}$ (g/cm <sup>3</sup> )					
HIGH	0.466 ± 0.033	0.449 ± 0.035	0.474 ± 0.030	<b>+0.025(5.5%)</b>	<b>0.025</b>
MID	0.529 ± 0.033	0.524 ± 0.027	0.531 ± 0.035	+0.007(1.3%)	0.477
LOW	0.505 ± 0.039	0.529 ± 0.035	0.495 ± 0.034	<b>-0.034(-6.5%)</b>	<b>0.004</b>
Mean temperature of the period crucial for cell wall thickening (°C)					
HIGH (9–29 Aug)	9.6 ± 1.2	8.8 ± 1.0	10.0 ± 1.2	<b>+1.2</b>	<b>0.002</b>
MID (22 Aug–11 Sep)	9.5 ± 1.5	8.4 ± 1.7	9.9 ± 1.2	<b>+1.5</b>	<b>0.005</b>
LOW (5–25 Sep)	9.6 ± 1.5	9.1 ± 2.0	9.8 ± 1.2	+0.7	0.244
Day of temperature transition below +9.5°C threshold (day of year)					
HIGH	233 ± 10	226 ± 11	235 ± 8	<b>+9</b>	<b>0.006</b>
MID	246 ± 8	241 ± 8	248 ± 7	<b>+7</b>	<b>0.010</b>
LOW	261 ± 9	259 ± 10	262 ± 9	+3	0.271



## Supplementary materials

### 1 Accessorial Calculations and Statistics for Anatomical Traits' Chronologies

#### 1.1 Normalization of tracheidograms

Normalization procedure operates on raw tracheidogram, which is a sequence of measured values of certain cell parameter for each cell in the ring radial file  $\{X_i\}$ ,  $i = 1, \dots, N$ , where  $X$  is cell parameter (e.g.,  $D$  or  $CWT$ );  $N$  is number of cells in measured radial file. Before standardization, we had to select certain number of cells  $c$ , which serves as number of narrow zones within tree ring. Selection is performed subjectively, taking into account trade-off between resolution and quality. In the study area, 15 cells showed reliable results (Babushkina et al. 2019; Belokopytova et al. 2019).

Procedure consists of two steps. Firstly, raw tracheidogram is stretched  $c$  times in the intermediate sequence  $\{X_i^*\}$ :

$$\{X_i^*\} = \underbrace{X_1, \dots, X_1}_c, \underbrace{X_2, \dots, X_2}_c, \dots, \underbrace{X_N, \dots, X_N}_c, \quad i = 1, \dots, N \cdot c.$$

Secondly, intermediate sequence is compressed into final normalized tracheidogram  $\{\hat{X}_i\}$ ,  $i = 1, \dots, c$ , where

$$\hat{X}_i = \frac{1}{N} \sum_{j=N \cdot (i-1) + 1}^{N \cdot i} X_i^*.$$

#### 1.2 Frequency distribution of cell tangential diameter T

Cell tangential diameter  $T$  was measured for sub-sample of randomly selected tree rings, one ring per each tree (i.e., 5 rings per site, 15 rings total). In each ring, the same 5 radial files of tracheids were measured as in measurements of  $D$  and  $CWT$ . Total number of measurements was 1570 cells. To analyze frequency distribution, histogram was plotted (Figure S1). Normality was tested with Shapiro-Wilk  $W$  test (Shapiro et al. 2012).

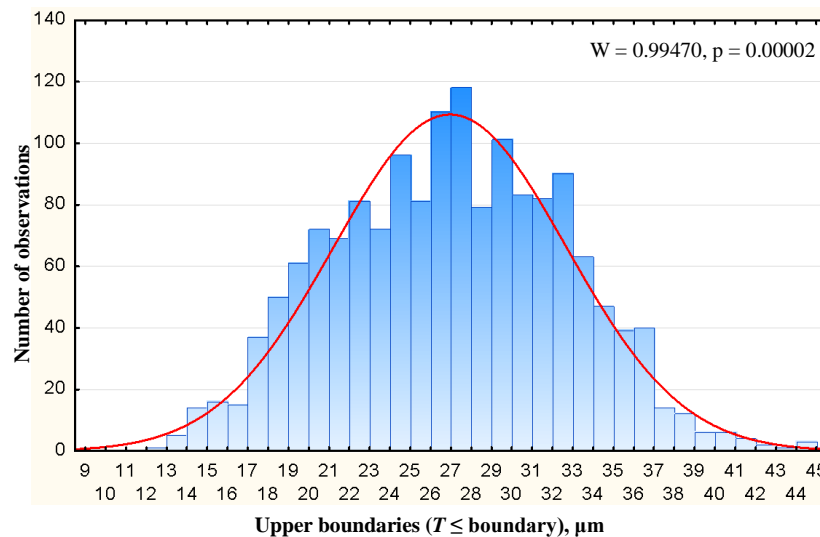


**Figure S1** Frequency distribution of  $T$ . Red line represents expected normal distribution

#### 1.3 Robustness statistics of site anatomical traits' chronologies

Mean inter-series correlation coefficient ( $\bar{r}$ ) and expressed population signal ( $EPS$ ) were

calculated for each site chronology of  $CWT_{max}$ ,  $\Sigma CWA$ , and  $\rho_{mean}$  (Table S1; Speer 2010).

**Table S1** Robustness statistics of site chronologies

Anatomical parameter	Site	$R\text{-bar}$	$EPS$
$CWT_{max}$	HIGH	0.290	0.671
	MID	0.345	0.729
	LOW	0.190	0.539
$\Sigma CWA$	HIGH	0.341	0.721
	MID	0.414	0.780
	LOW	0.182	0.526
$\rho_{mean}$	HIGH	0.468	0.815
	MID	0.350	0.729
	LOW	0.219	0.584

## References

Shapiro SS, Wilk MB, Chen HJ (1968) A comparative study of various tests for normality. Journal of the American statistical association 63(324): 1343-1372. <https://doi.org/10.2307/2285889>  
Speer JH (2010) Fundamentals of Tree-Ring Research. Tucson: University of Arizona Press, p 368.

## 2 Search for Optimal Window Width of Temperature Moving Series Used in Dendroclimatic Analysis of $CWT_{max}$

When using short-term moving series of climatic variables for a detailed analysis of the climate–growth relationships, a methodological question arises of the optimal window width  $W$  for the averaging/summarizing procedure. For example, we have previously successfully used  $W = 10, 11, 15, 20,$  and  $21$  days to analyze the correlations between climatic variables and chronologies of the crops yield,  $TRW$  and anatomical characteristics of conifers in previous studies (Demina et al. 2017; Arzac et al. 2018; Babushkina et al. 2018a, 2018b, 2019; Belokopytova et al. 2018, 2019).

In order to identify the most appropriate window width in this particular case, we performed the exhaustive search in range  $W = 1...25$  days, where for each  $W$  correlations between  $CWT_{max}$  and moving averaged series of temperature in August–September were calculated (Figure S2). Analysis of the correlation coefficients showed that at the HIGH and MID sites, the window width  $W = 21$  days used in the previous study gives the best results (Table S1). It should also be noted that within the identified periods of the maximum temperature influence on  $CWT_{max}$ , high correlations are also observed with smaller window widths (areas between dashed lines in Figure S2). However, at the LOW site, the maximum correlation is reached at  $W = 17$  days, while climate–growth relationships themselves are weaker than at other elevations.

**Table S2** Maximum correlations between  $CWT_{max}$  site chronologies and moving average temperature series

Site	$R_{max}^*$	$W^{**}$	Period (calendar date / day of year)		
			onset	center	offset
HIGH	0.378	21	9 Aug / 221	19 Aug / 231	29 Aug / 241
MID	0.393	21	22 Aug / 235	1 Sep / 245	11 Sep / 255
LOW	0.312 (0.291)	17 (21)	7 Sep / 251 (5 Sep / 249)	15 Sep / 259	23 Sep / 267 (25 Sep / 269)

\* All correlations are significant at the level  $p < 0.05$ .

\*\* At the LOW site, correlations are shown not only for maximal value of  $R_{max}$ , but also for  $W = 21$  days. A value of  $R_{max}$  at this window width is not significantly different from a value at  $W = 21$  days, thus all further calculations are performed for the uniform  $W = 21$  days for all three sites.

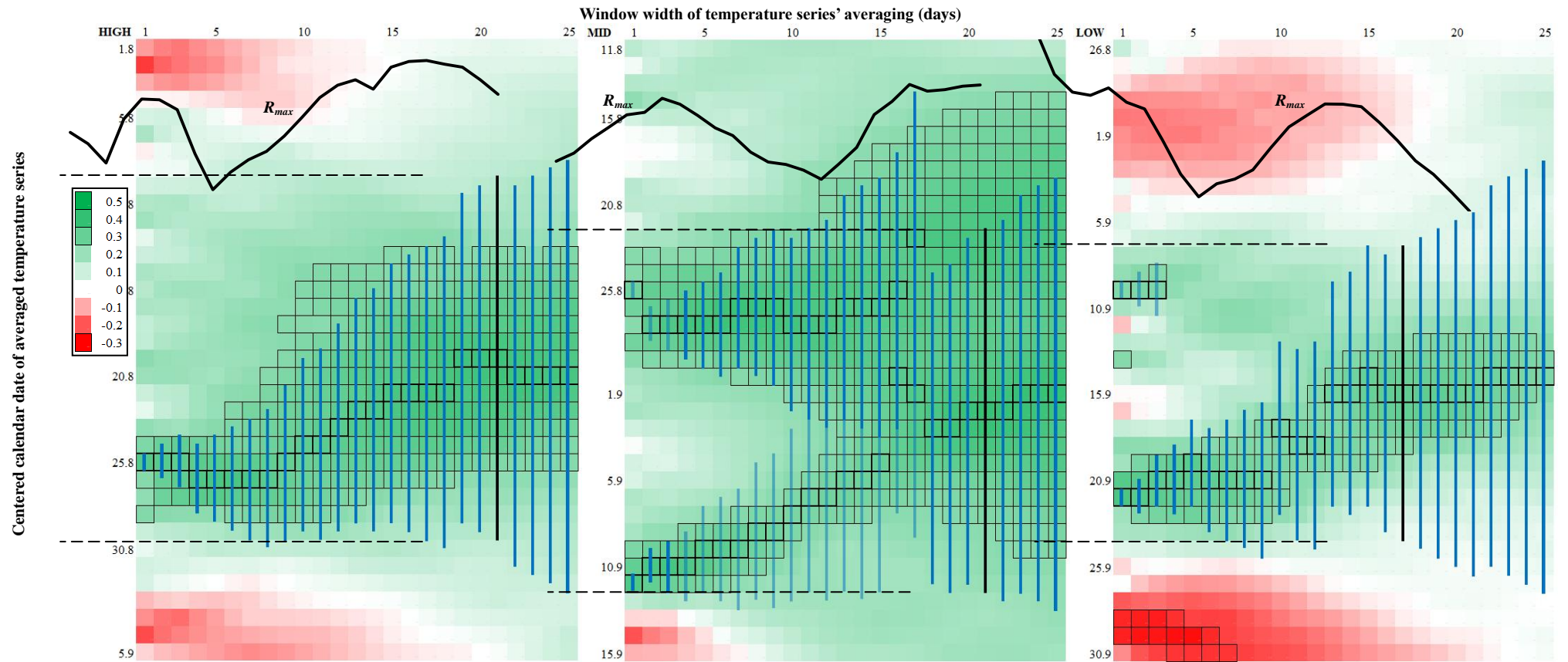


**Figure S2** Correlations of *CWTmax* chronologies at the LOW, MID, and HIGH sites with temperature series averaged using window widths  $W=1\dots25$  days from daily data. A color gradient marks values of correlation coefficients (see the scale in legend); correlations significant at  $p < 0.05$  are marked with borders ( $\square$ ). The maximum correlation  $R_{max}$  for each  $W$  is marked with bold borders and with a vertical bar indicating calendar period of averaging for respective temperature series. If correlations have two significant maxima for particular  $W$ , the secondary maximum is marked with a lighter bar. A curve of the function  $R_{max}(W)$  is shown in the top part of each diagram, the highest value of  $R_{max}$  corresponds to the crucial period of temperature influence marked with a black bar, and dates of its beginning and ending are marked with horizontal dashed lines

### 3 Verification of the Elevational Lapse Rate of Temperature for the Study Area

The empirical research showed that the actual lapse rate of air temperature with elevation in the mountains may vary depending on the landscape (e.g., the configuration / orientation of the slopes, in consequence of them the most probable wind directions, etc.) and change with the season (Maurer et al. 2002; Hamlet and Lettenmaier 2005; Chae et al. 2012; Wypych et al. 2018). Therefore, when analyzing the course of temperature on an elevational transect with the availability of long-term data from only one weather station (i.e. one elevation), it is necessary to verify a temperature lapse rate before its application.

We assumed that due to the regulation of the growth season duration by temperature, the formation of the most thick-walled tracheids within one population of conifer trees (meaning one ecotype of species and common genetic pool) should be observed at similar temperatures regardless of elevations. For open air, the average temperature lapse rate is  $\Delta T_{100} = -0.65^{\circ}\text{C}$  per 100 m, this value was taken as the initial one. The seasonal temperature dynamics at the Cheryomushki weather station was smoothed by the 21-day moving average, and then averaged over the period of anatomical measurements 1965-2014. A resulting curve of seasonal temperature variation was adjusted for each sampling site, using correction factors calculated from the lapse rate and the difference in elevation between the site and the weather station:

$$\begin{aligned} \Delta T_{\text{site}} &= \Delta T_{100} \cdot (h_{\text{site}} - h_{\text{station}}) / 100, \text{ i.e.} \\ \Delta T_{\text{LOW}} &= -0.65 \cdot (520 - 330) / 100 = -1.24^{\circ}\text{C}; \\ \Delta T_{\text{MID}} &= -0.65 \cdot (960 - 330) / 100 = -4.10^{\circ}\text{C}; \\ \Delta T_{\text{HIGH}} &= -0.65 \cdot (1320 - 330) / 100 = -6.44^{\circ}\text{C}. \end{aligned}$$

Verification was performed by comparison of corrected temperatures in the beginning, middle, and ending of the 21-day period when correlations between  $CWT_{\text{max}}$  and  $T$  are maximal at each site (Figure S3, Table S2). These temperatures don't have any elevational gradients with used correction factors, which supports choice of the lapse rate value  $\Delta T_{100} = -0.65^{\circ}\text{C}$  per 100 m for the considered sampling sites and season (August–September).

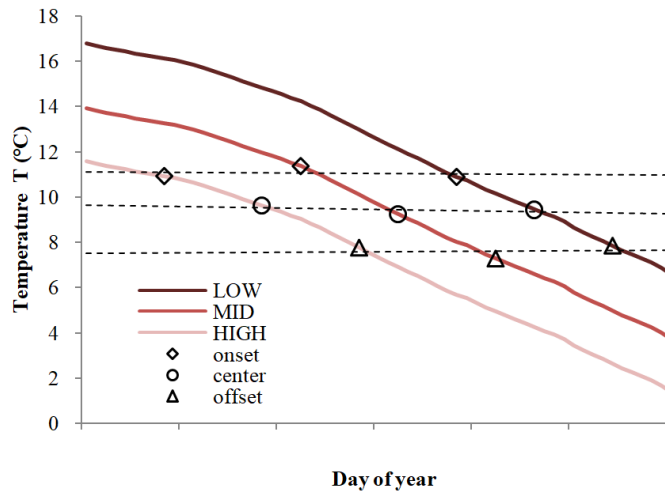


**Figure S3** Dynamics of temperature in August–September at three sampling sites averaged over period 1965-2014. Temperatures in the beginning (diamonds), middle (circles), and ending (triangles) of the period crucial for  $CWT_{\text{max}}$  are marked

**Table S3** Corrected temperature (*mean ± stdev*) at the sampling sites during the 21-day period of maximal correlation between  $T$  and  $CWT_{\text{max}}$ , averaged over 1965-2014

Site	Temperature $T$ ( $^{\circ}\text{C}$ )			
	daily at the dates of			whole period
	onset	center	offset	
HIGH	$11.0 \pm 2.9$	$10.2 \pm 2.8$	$7.7 \pm 3.0$	$9.6 \pm 1.2$
MID	$11.8 \pm 2.8$	$9.5 \pm 3.2$	$7.7 \pm 3.3$	$9.5 \pm 1.5$
LOW	$11.0 \pm 3.5$	$9.3 \pm 2.9$	$7.7 \pm 3.5$	$9.6 \pm 1.5$

#### 4 Analysis of the Dates of Temperature Transition Under Certain Thresholds at the End of the Growth Season

Taking into account the obtained temperature estimations during the period of its maximum effect on CWTmax (Table S2), the analysis of the dates of temperature crossing certain thresholds was performed for the threshold values  $T_{thr}$  from +8.5 to +10.5°C with step 0.5°C. Series of the dates of this transition were obtained with different techniques and correlated with CWTmax site chronologies (Table S3). The widely used method for estimating temperature transition through the threshold by the last occurrence of  $T < T_{thr}$  in spring and the first occurrence of  $T > T_{thr}$  in autumn (Pedlar et al. 2015) is not applicable in the study area, because there daily temperatures can drop lower than these  $T_{thr}$  values even in the middle of the warm season (e.g. down to +4°C at the HIGH site in July). Therefore, we used other techniques: the day before the first 5-day period of  $T < T_{thr}$  (Frich et al. 2002), more complex official agroclimatic technique used in Russia (Rosgidromet 2010), and estimation of the transition date from temperature series smoothed by a 21-day moving average as the last day when smoothed  $T$  is above the threshold (cf. Christidis et al. 2007).

At two of the three sites, the best correlations with CWTmax are observed for +9.5°C threshold value and date calculation according to the Russian technique. It should be noted, that the average date of this transition over period 1965-2014 is consistently 1-2 days after the middle of the period of maximum temperature influence on CWTmax. Also, the average temperature of this period at all sites is close to 9.5°C. It leads us to the tentative conclusion that a mean temperature of the period of maximum correlations between temperature and chronology of a certain tree-ring parameter can be used as an estimation of the temperature threshold regulating the corresponding physiological process.

When using the Russian technique for obtaining series of transition dates, their standard deviations are in the range of 7.7–10.7 days. It means that in this study, the transition dates for +9.5°C threshold fluctuate within the obtained 21-day period of the maximum temperature influence in at least 67% of years. It would be interesting to check this pattern (the optimal window width of dendroclimatic correlation matching with the variation range of a threshold transition date) on other parameters of tree rings and temperature thresholds involved in their regulation.

**Table S4** Dates of temperature transition through certain thresholds calculated with different techniques, and their correlations with CWTmax

Site	$T_{thr}$ , °C	Date of transition in August–September, estimated as		
		last day of Av21 $T > T_{thr}$	day before first 5-day period of $T < T_{thr}$	in the official Russian agroclimatic technique*
HIGH	10.5	224 ± 11 / 0.218	227 ± 12 / 0.018	225 ± 11 / <b>0.238</b>
	10.0	229 ± 9 / 0.189	230 ± 10 / 0.130	228 ± 10 / <b>0.260</b>
	9.5	232 ± 8 / 0.231	232 ± 10 / 0.148	233 ± 10 / <b>0.294</b>
	9.0	235 ± 7 / <b>0.289</b>	235 ± 8 / 0.178	235 ± 9 / 0.199
	8.5	237 ± 7 / <b>0.281</b>	237 ± 7 / 0.145	238 ± 8 / 0.091
MID	10.5	239 ± 7 / <b>0.274</b>	240 ± 9 / 0.197	239 ± 8 / 0.114
	10.0	242 ± 7 / 0.170	243 ± 9 / 0.056	243 ± 8 / <b>0.268</b>
	9.5	245 ± 7 / <b>0.266</b>	247 ± 10 / 0.026	246 ± 8 / <b>0.340</b>
	9.0	247 ± 7 / <b>0.284</b>	248 ± 10 / 0.071	248 ± 8 / <b>0.340</b>
	8.5	249 ± 7 / 0.207	251 ± 10 / 0.130	251 ± 9 / <b>0.250</b>
LOW	10.5	253 ± 7 / 0.110	255 ± 11 / <b>0.278</b>	257 ± 9 / 0.059
	10.0	256 ± 7 / 0.172	258 ± 11 / 0.190	259 ± 9 / 0.092
	9.5	259 ± 7 / 0.112	259 ± 10 / 0.126	261 ± 9 / 0.142
	9.0	262 ± 7 / 0.140	262 ± 10 / 0.086	264 ± 10 / 0.173
	8.5	264 ± 8 / 0.103	264 ± 11 / 0.143	267 ± 9 / <b>0.251</b>

Numerator is *mean ± stdev* (DOY) of date; denominator is correlation of date series with CWTmax. Bold correlations are significant at  $p < 0.05$ .

\* The first day of the first continuous period of daily  $T < T_{thr}$  with  $\Sigma|T - T_{thr}|$  more than for any subsequent period of  $T > T_{thr}$ .

## 5 Scaling of Additional Wood Matter Deposition at the Expense of Anatomical Structure Change

Inventory data of spruce in the mixed stands by the end of 2010 obtained from the National Park “Shushensky Bor” (Table S4) were used as initial data source for calculations. As it was calculated in the previous study (Babushkina et al. 2018a), the average radial growth of spruce is 0.72, 0.99, and 2.25 mm per year at the HIGH, MID, and LOW sites, respectively. If we take as an example the average trunk radii at the sites according to the inventory data, we receive the basal area of 314, 531 and 616 cm<sup>2</sup>, respectively. With these initial data, the average radial growth will correspond to the annual basal area increment of 4.54, 8.12, and 19.95 cm<sup>2</sup>.

**Table S5** Inventory data of spruce in the mixed stands

Site	Area (ha)	Mature trees of spruce		
		Wood volume, (m <sup>3</sup> )	Mean age (years)	Mean diameter (cm)
HIGH	29.7	119	150	20
MID	37.7	792	200	26
LOW	1.1	49	100	28

The total cell wall area  $\Sigma CWA$  is calculated for a single radial file in a normalized tree ring consisting of 15 cells, i.e. approximately rectangular area with width of average cell tangential size (27  $\mu\text{m}$ ) and length of  $\Sigma D = 15 \cdot D_{\text{mean}} \approx 0.4$  mm. Therefore, to estimate the increase in the amount of deposited wood matter at different spatial scales, a recalculation is required for actual increments and areas. Comparing the formation of the anatomical structure of wood under typical climatic conditions before and after 1980 (that is, using the average  $\Sigma CWA$  values for the corresponding sub-periods), we obtain the average total wall area around the entire circumference of the ring 1.32, 2.68 and 6.51 cm<sup>2</sup> when it is formed under the conditions existed before local warming, and 1.41, 2.86 and 6.61 cm<sup>2</sup> under the conditions existing after it. It means that, disregarding age trends in the radial increment (we can do it because in the study area, spruce population has a stable growth with a wide variety of tree ages including saplings), for an average tree at the site, the local climate change leads to an increase in the total cell wall area formed over the year by 0.08 cm<sup>2</sup> at the HIGH site, 0.18 cm<sup>2</sup> at the MID site, and 0.10 cm<sup>2</sup> at the LOW site.

Estimating the volume of spruce wood per unit of the forest area at each site (4 m<sup>3</sup>/ha at the HIGH site, 21 m<sup>3</sup>/ha at the MID site, and 45 m<sup>3</sup>/ha at the LOW site) and the rate of its accumulation (dividing it by the average tree age) from inventory data, we obtain an average annual wood accumulation of 0.027, 0.105 and 0.445 m<sup>3</sup>/ha per year just for spruce (not accounting for other tree species in the stands). When this wood is formed in the conditions of a changed local climate, due to anatomical changes this volume contains 1650, 7101 and 6755 cm<sup>3</sup> of wood matter more than under the conditions before warming, i.e. by 2.5, 10.9 and 10.3 kg per hectare every year.